Image Processing Techniques for Glaucoma Detection Using the Cup-to-Disc Ratio

Chalinee Burana-Anusorn[1], Waree Kongprawechnon[1], Toshiaki Kondo[1], Sunisa Sintuwong[2] and KanokvateTungpimolrut[3]

[1] School of Information, Computer, and Communication Technology
Sirindhorn International Institute of Technology, Thammasat University

[2] Mettapracharak Eye Center, Mettapracharak (Wat Raikhing) Hospital

[3] National Electronics Computer and Technology Center, NSTDA

Correspondence:
Chalinee Burana-Anusorn
School of Information, Computer, and Communication Technology Sirindhorn International Institute of Technolgy, Thammasat University.
Email: taw 34@hotmail.com

Abstract

Glaucoma is the second leading cause of permanent blindness worldwide. Early detection of glaucoma can limit the disease progression. The ratio of the size of the optic cup to the optic disc, also known as the cup-to-disc ratio (CDR), is one of the important clinical indicators of glaucoma, and is currently determined manually by trained ophthalmologists, limiting its potential in mass screening for early detection. In this paper, the authors propose a method to calculate the CDR automatically from non-stereographic retinal fundus photographs taken from a NIDEK AFC-230, which is a non-mydriatic auto fundus camera. To automatically extract the disc, two methods making use of an edge detection method and variational level-set method are proposed in the paper. For the cup, color component analysis and threshold level-set method are evaluated. To reshape the obtained disc and cup boundary from our methods, ellipse fitting is applied to the obtained image. A set of 44 retinal images obtained from Mettapracharak Hospital, Nakhon Pathom Thailand is used to assess the performance of the determined CDR to the clinical CDR, and it is found that our proposed method provides 89% accuracy in the determined CDR results.

Keywords: Glaucoma, Cup-to-disc ratio, Fundus retinal image, Level set, Component analysis

1. Introduction

Glaucoma is a chronic and irreversible neurodegenerative disease. Patients with early glaucoma do not usually have any visual signs or symptoms. Progression of the disease results in loss of peripheral vision and patients may complain of tunnel vision (being only able to see centrally). Advanced glaucoma is associated with total blindness.

According to World Health Organization, glaucoma is the second leading cause of blindness; it is responsible for approx- imately 5.2 million cases of blindness (15% of the total burden of world blindness) [1] and will increase to 11.2 million people by 2020. In Thailand, glaucoma is found to be prevalent in 2.5-3.8% of the Thai population or approximately 1.7-2.4 million people [2]. Hence, a timely and precise early detection of glaucoma plays a key role for preventing irreversible damage in eyes.

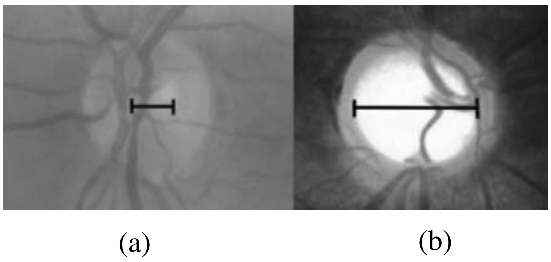

Fig. 1. a) Normal optic nerve head with small optic cup. b) Glaucomatous optic nerve head. The hole is larger, corresponding to the loss of nerve fibers.

Currently, an important indicator of glaucoma is CDR, defined as the ratio of the vertical height of the optic cup to the vertical height of the optic disc. Optic nerve cupping progresses as the cup becomes larger (Figure 1(b)) in comparison to the optic disc as shown in Figure 1(a). A cup to disc ratio value that is greater than 0.65 is generallyconsidered to be suspicious for glaucoma[3].

Many studies have been reported previously on the automatic segmentation of the optic disc and cup from retina fundus images. Many studies proposed a disc detection scheme using variational level-set segmentation and then, using threshold level-set segmentation for cup detection [4][5][6]. This method uses an elliptical fitting post-processing to handle deformation caused by blood vessels. The method presented in [7] uses manual threshold analysis, color component analysis and ROI (Region of Interest) based segmentation for the detection of the cup. For the cup, the component analysis method is used.

2. Problem Statement

An early detection of glaucoma is particularly significant since it allows timely treatment to prevent major visual field loss and prolongs the effective years of usable vision. The diagnosis of glaucoma can be done through measurement of CDR (cup-to-disc ratio). Currently, CDR evaluation is manually performed by trained ophthalmologists or expensive equipment such as Heidelberg Retinal Tomography (HRT). However, CDR evaluation by an ophthalmologist is subjective and the availability of HRT is very limited. Thus, this paper proposes an intuitive, efficient and objective method for automatically classifying digital fundus images into either normal or glaucomatous types in order to facilitate ophthalmologists.

3. Methodology

To calculate the vertical cup to disc ratio (CDR), the optic cup and disc first have to be segmented from the retinal images. Figure 2 depicts the framework for building the proposed detection system.

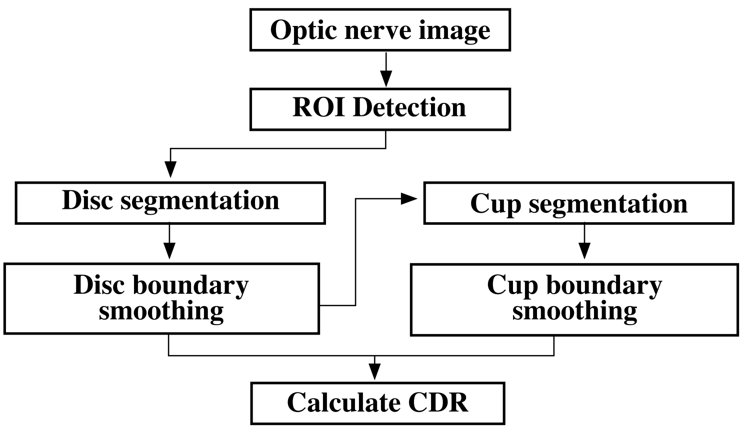

Fig. 2. Retina image processing framework for cup-to-disc ratio (CDR) detection in glaucoma analysis.

3.1 Region of Interest Detection

To calculate the vertical cup to disc ratio (CDR), the optic cup and disc first have to be segmented from the retinal images. Figure 2 depicts the framework for building the proposed detection system.

In order to extract the optic disc and cup, each retinal fundus image has been captured using a high resolution retinal fundus camera and saved as a 3072 x 2048 high-resolution digital image, as shown in Figure 3(a). Thus, the region of interest (ROI) around the optic disc must first be delineated. Correctly identifying the ROI results in a small image, speeding up the calculation of the CDR, since its size is usually less than 11% of the entire retinal fundus image. ROI localization will require less human intervention and has potential for mass automated screening. In this paper, the set of fundus images are firstly examined, and it is found that the optic disc region is usually of a brighter pallor or higher color intensity than the surrounding retinal area. The fundus images with the highest intensity are selected as potential candidates for the optic disc center, as shown in Figure 3(b). The intensity-weighted centroid method[8] is proposed to find an approximate ROI centre. The boundary of the ROI is defined as a rectangle around the ROI centre with dimensions of twice the typical optic disc diameter, and is used as the initial boundary for the optic disc segmentation, as shown in Figure 3(c). The ROI is returned as an image of size 480x750 pixels as shown in Figure 3(d).

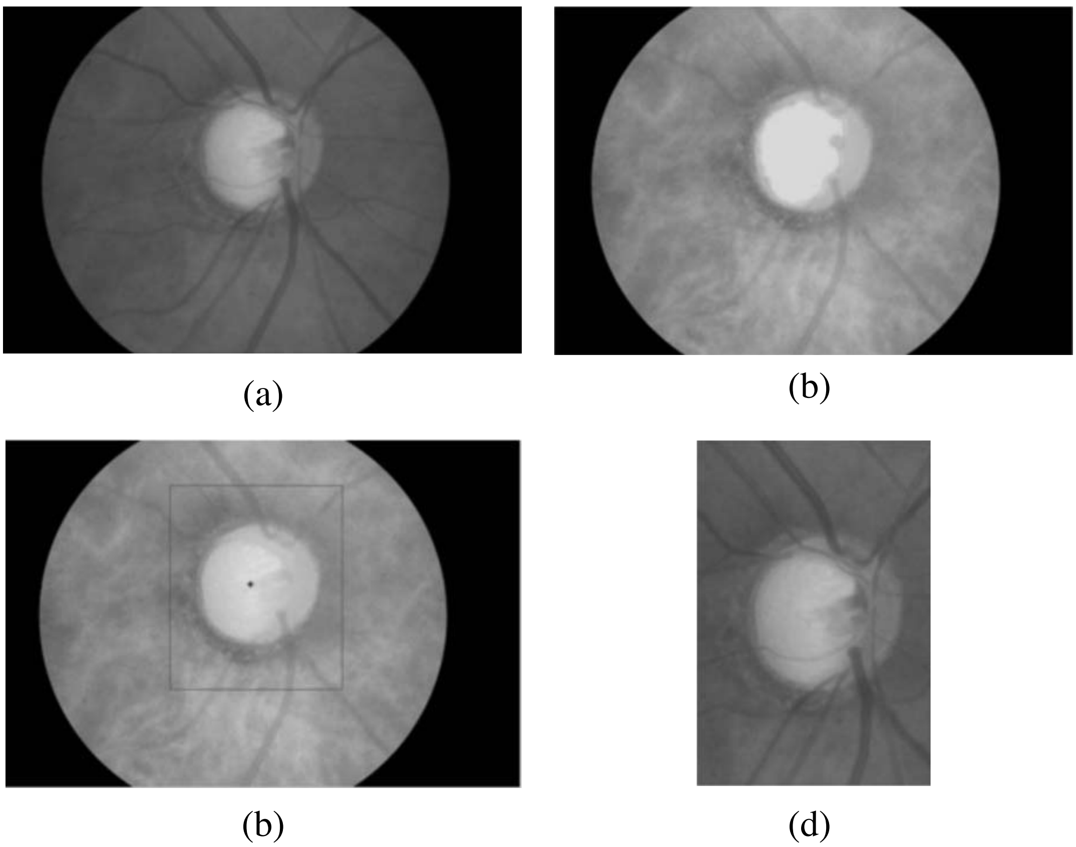

Fig. 3. a) Input image of size 3072 x 2048 pixels b) A brighter pallor detected (blue area) c) ROI localization d) ROI image of size 480 x 750 pixels.

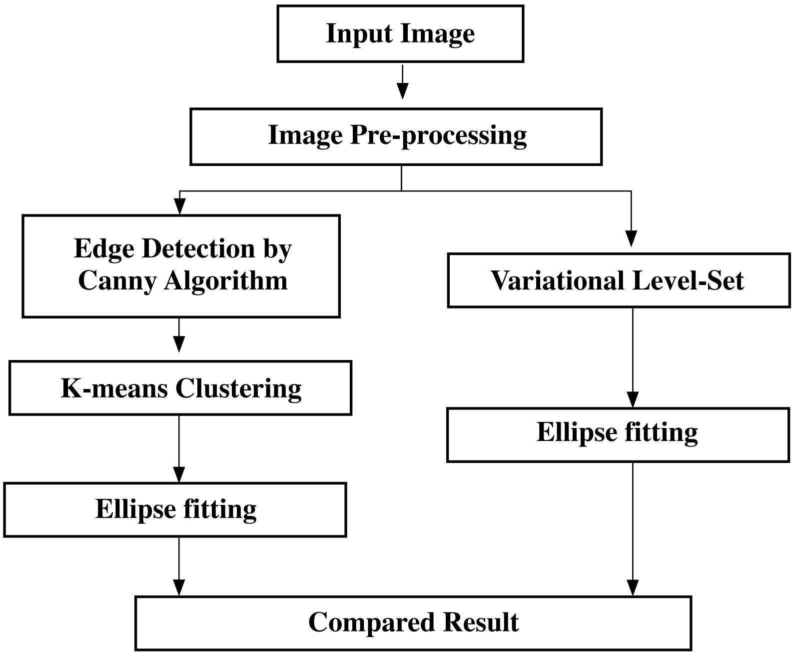

Fig. 4. The framework for optic disc segmentation.

3.2 Optic Disc Segmentation

To detect an optic disc boundary, image pre-processing is introduced. Figure 4 shows a simplified workflow of optic disc segmentation.

Firstly, a coarse localization of optic disc region is presented using the red channel. The red component is utilized as it is found to have higher contrast between the optic disc and non-optic disc area than for other channels.To remove the blood vessels, a morphological closing operation is performed. Closing is defined as dilation followed by erosion, and it tends to enlarge the boundaries of foreground regions in an image and shrink background color holes in such regions. The size of structuring element chosen in this paper is 20 by 20 pixels because this size is larger than the width of major vessels. After performing the closing operation, a median filter is applied to further smoothen the obtained image. The outputs of the image pre-processing are shown in Figure 5.

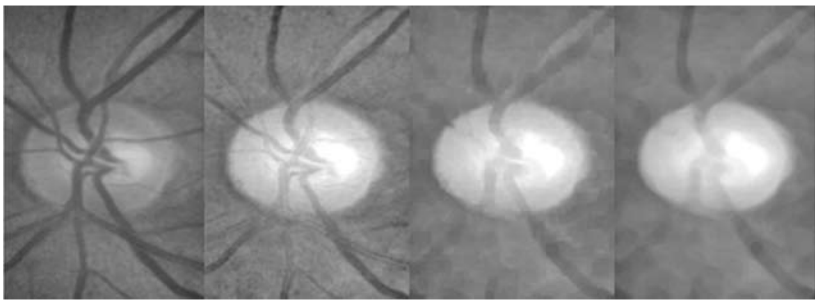

(a) (b) (c) (d)

Fig. 5. a) Input Image b) Red channel c) Closing operation and d) Median filter.

After the image pre-processing is performed, two techniques for extracting a disc boundary are introduced: Edge Detection Approach and Variational Level-Set Approach.

3.2.1 Edge Detection Approach

In this method, the optic disc is extracted by the edge command in MATLAB. The Canny method is specified for edge detection because the Canny algorithm can detect edges with noise suppressed at the same time. This method uses two thresholds, to detect strong and weak edges, and it includes the weak edges in the output only if they are connected to strong edges. The optimum threshold of the each input retinal image is found to be different due to the variant intensities in each image.

Although the optimum threshold of the input retinal image has been adjusted for several times to detect only a disc boundary, the edge command still detects the blood vessel inside the optic disc and also outside the optic, disc as shown in Figure 7(b). In order to extract only a disc boundary, the edge image has to be classified into three groups based on the distance from the center of the optic disc as shown in Figure 6 and Figure 7(a). This classification is achieved by performing k-means clustering to the edge of the image (Figure 7(b)). K-means clustering is a method of cluster analysis which aims to partition n observations into k clusters in which each observation belongs to the cluster with the nearest mean [9]. Then, the group that contains only edge detection of a disc boundary is selected, and the noise can be rejected as shown in Figure 7(c).

After that, the application of direct ellipse fitting is used to obtain boundaries in order to find a smoother contour. The outputs are shown in Figure 7(d).

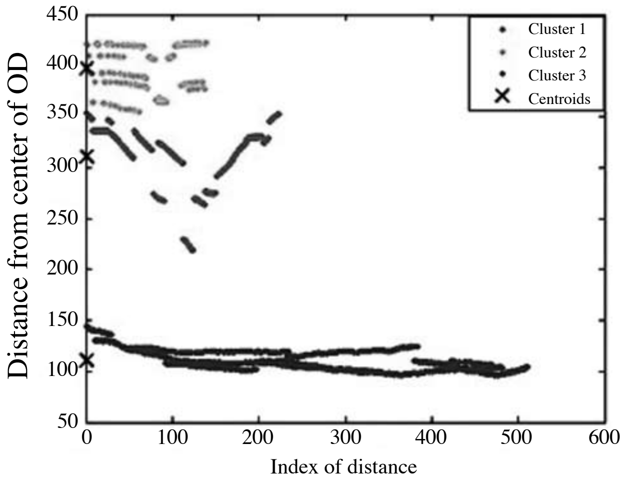

Fig. 6. Graph shows three clusters from edge detection data.

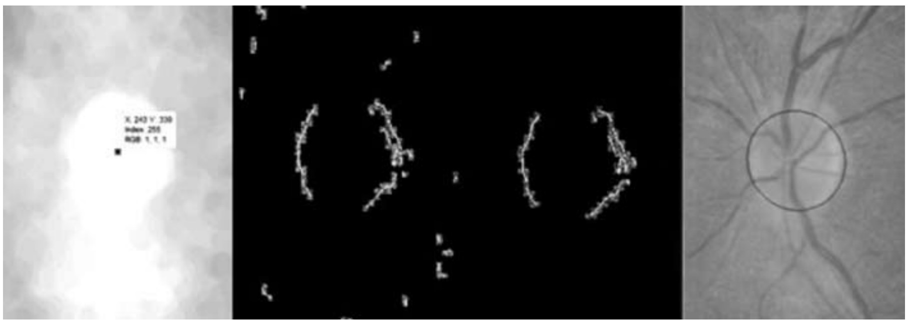

(a) (b) (c) (d)

Fig. 7. a) Input image after performing the image pre-processing with the center of an optic disc b) Edge detection c) The result after noise is rejected d) Disc boundary smoothing.

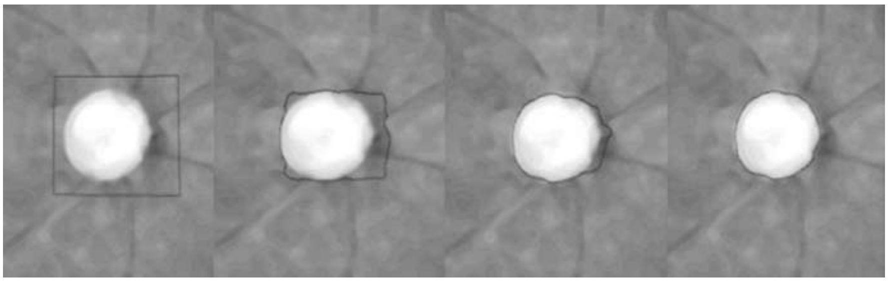

(a) (b) (c) (d)

Fig. 8. Sample evolution results at different iterations. a) 1st b) 120th c) 250th and d) 300th iterations.

3.2.2 Variational Level-Set Approach

The variational level- set algorithm has been widely used as a global approach for the optimization of active contours for the segmentation of objects of interest from the background [6][7]. In this study, this method is employed by initializing a curve centered at the detected optic disc location. The curve is evolved based on the average intensity value inside and outside the curve. The curve evolution always converges to the optic disc boundary irrespective of the shape or size of the initial contour. Figure 8 shows a sample evolution result where the initial curve is a rectangle.

3.3 Optic Cup Segmentation

Compared to the extraction of the optic disc, optic cup segmentation is more challenging due to a cup's inter weavement with blood vessels and surrounding tissues. This study presents two approaches for cup segmentation, which are the color component analysis approach and threshold level set approach.

3.3.1 Color Component Analysis Approach

In the color component analysis method, RGB components of the input images (Figure 9(a)) are analyzed, and it is found that the optic cup is more easily discriminated in the green image because the visibility and contrast of the optic cup is superior and its pixels are of higher intensities, while the neuroretinal rim and the retinal vessels are often of lower intensities. Thus, the green color is detected with some threshold value, and the result is shown in Figure 9(b) as the white area. The optimum threshold value in each image is the top 1/3 of the grayscale intensity. The next step is to use morphological opening operation in order to remove noise around the cup region as shown in Figure 9(c) and, then the edge detection (Figure 9(d)) and ellipse fitting is proposed to obtain the cup boundary smoothing. The outputs are shown in Figure 9(e).

(a) (b) (c) (d) (e)

Fig. 9. a) Input image b) Color green detected c) Morphological opening operation d) Edge detection e) Cup boundary smoothing.

3.3.2 Threshold Level Set Approach

In this approach, the green channel of the input image (Figure 11(a)) is selected as the basis for further segmentation due to the optimum observed contrast between the cup and disc boundaries in this channel. Then the normalized cumulative histogram (Figure 10) of the green channel image is analyzed and a threshold value which segments out the pixels, corresponding to the top 1/3 of the grayscale intensity, is used to define the initial cup contour. The method to select the top 1/3 of the grayscale intensity is to find the threshold value from the normalized cumulative histogram and then compare it with all the intensity values of the input image. Then an intensity value is that is greater than the threshold value is selected, as shown in Figure 11(b). The next step is to use a morphological opening operation in order to remove noise around the cup region, as shown in Figure 11(c). Next, the intensity-weighted centroid method [8] is proposed to find an approximate initial point, as shown in Figure 11(d). This is found to give a good initial approximation for the initial cup region, as shown in Figure 11(e).

Then, a threshold level-set algorithm is applied to segment the optic cup. The principle of this method is similar to the variational level-set algorithm. Figures 12 a) through c) show sample evolution results at different iterations. Then an ellipse fitting application is proposed, to smooth and regulate the shape of segmented cup boundary, as seen in Figure 12(d).

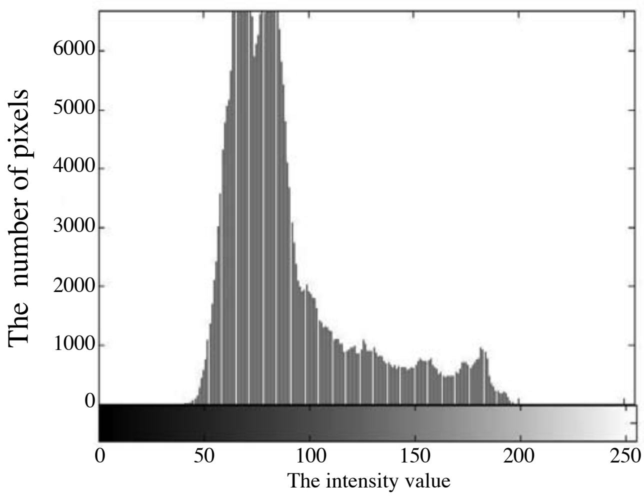

Fig. 10. The normalized cumulative histogram of the green channel image.

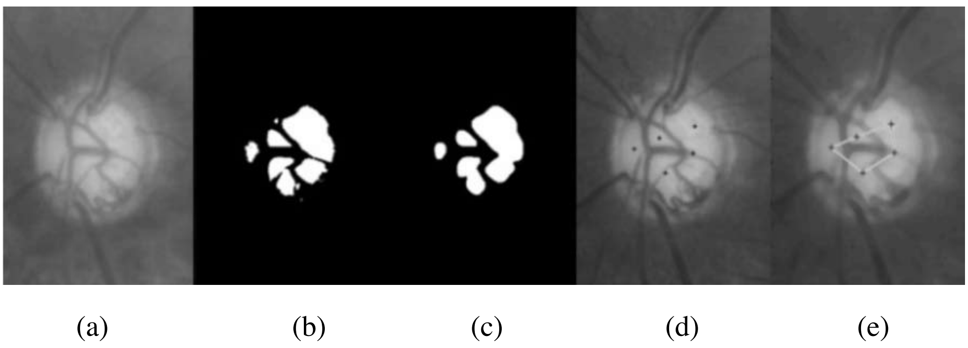

Fig. 11. a) Input image b) Color green detected c) Morphological opening operation d) The initial point of cup region e) The initial cup contour.

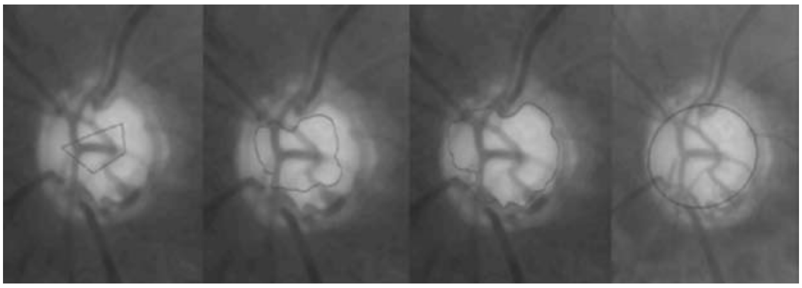

(a) (b) (c) (d)

Fig. 12. a) Input image b) Sample evolution results at different iterations (150th) c) 300th d) Cup boundary smoothing.

3.4 Ellipse Fitting for Optic Disc and Cup

The ellipse fitting algorithm can be used to smooth the disc and cup boundary. The mathematical representation is the conic equation of the ellipse.

$$F(a,x) = a \cdot x = ax^2 + bxy + cy^2 + dx + ey + f = 0 \tag{1}$$

where $a = [a\ b\ c\ d\ e\ f]^T$

and $x = [x^2\ xy\ y^2\ x\ y\ 1]^T$

$F(a;x_i)$ is called the algebraic distance of a point (x, y) to the conic F (a, x) = 0. Ellipse fitting is usually based on least square fitting algorithm which assumes that the best-fit curve of a given type is the curve that minimizes the algebraic distance over the set of N data points in the least squares sense, that is:

$$\sum_{i=1}^{N} F(x_i)^2 \tag{2}$$

B2AC (Direct Least Square Fitting Algorithm) [11] is chosen to fit the optic and cup because it minimizes the algebraic distance subject to a constraint, and incorporates the ellipticity constraint into the normalization factor. It is ellipse-specific, so that effect of noise (ocular blood vessel, hemorrhage, drusens, etc.) around the cup area can be minimized while forming the ellipse. It can also be easily solved naturally by a generalized eigensystem.

In B2AC, a quadratic constraint is set on the parameters to avoid trivial and unwanted solutions. The goal of B2AC is to search a vector parameter which contains the six co-efficients of the standard form of a conic. Minimizing the sum of the squared algebraic distance Da, can be solved by considering a rank-deficient generalized eigenvalue system,

$$D^T Da = \lambda Ca \tag{3}$$

where $D=[x_1 x_2\ \ldots x_n]^T$ is the n x 6 design matrix for n data points x(sub)i and C is the constraint matrix. The B2AC method further constrains the parameter vector a in such a way that it forces the conic to be an ellipse through imposing the equality constraint:

$$4ac - b^2 = 1 \tag{4}$$

Where a, b, c are the first three coefficients of the conic. This quadratic constraint can be expressed in matrix form $a^T Ca=1$. The constrained ellipse fitting problem reduces to minimize $\|Da\|^2$ subject to the constraint $a^T Ca=1$. It is possible to rewrite Equation (3) as:

$$Sa = \lambda Ca \tag{5}$$

where S is the scatter matrix, D^TD and this system can readily be solved by considering the generalized eigenvectors of Equation (5). The solution of the eigensystem (Equation 5) gives six eigen-value-eigenvector pairs (λ_i, u_i). By considering the minimization $\|Da\|^2$, subject to the constraint (Equation 4) there is only one solution, which corresponds, by virtue of the constraint, to an ellipse.

4. Result and Analysis

To evaluate the performance of our approach, we obtained 44 fundus images from Mettapracharak hospital conducted by the Mettapracharak Eye Center. There are 28 of the retinal images from normal patients, with no clinical signs of glaucoma, and 16 of the retinal images are from patients with glaucoma. At this point, the set of 44 test images are processed using the approach outlined earlier in order to obtain the CDR value, $CDR_{Automated}$. For the ground truth, the optic cup and disc boundaries are assessed and annotated by a senior ophthalmologist based on the retinal fundus images, and the vertical CDR for each image, CDR_{Clinic}, was determined. The evaluation of the performance of our approach is divided into 3 parts, which are the performance of the optic disc boundary detection, the performance of the optic cup boundary detection, and the vertical cup-to-disc ratio (CDR).

4.1 The optic disc boundary detection

The 44 images are processed using our proposed approach, edge detection, approach and variational level-set approach to obtain the disc diameter, $Disc_{Edge}$ and $Disc_{Level-Set}$ for each eye. The percentage error is defined as:

$$\% \text{ Error} = \left| \frac{Disc_{Clinic} - Disc_{Edge/Level-Set}}{Disc_{Clinic}} \right| \tag{6}$$

The average disc detection error of edge detection method and variational level-set method is 3.75% and 5.42%, respectively. A graph is plotted for the clinical disc diameter with the detected disc diameter from the two methods, as shown in Figure 13.

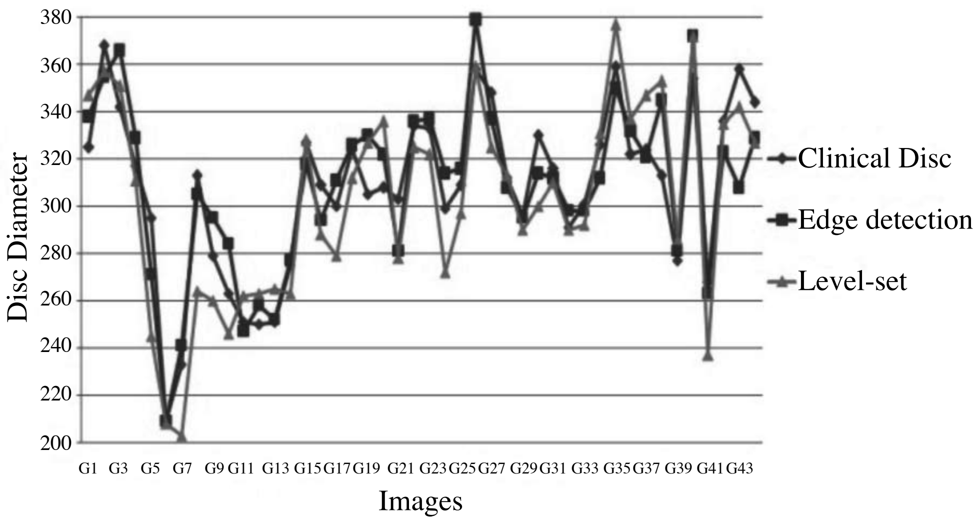

Fig. 13. Comparison of clinical disc detection and disc segmentation from edge detection method and variational level-set method.

It can be seen that the edge detection approach provides a better result when compared with the variational level-set method. In addition, the performance of the edge detection method is easier to understand in terms of MATLAB code. The time for running MATLAB code of this method is about 10 seconds per image while the variational level-set method takes about 5 minutes per image. However, the performance of the variational level- set method is more automated than the edge detection method because, in the edge detection method, we have to adjust the threshold value of the edge command for each input image due to the variable intensities of the input data. As a result of running time and ease of understanding, the edge detection method is chosen for CDR calculation.

4.2 The optic cup boundary detection

The same sets of images are processed using color component analysis method and threshold level-set method for cup segmentation. To evaluate the performance of the approach, the percentage error between the results obtained from the automated calculation $Cup_{Color/Level\text{-}set}$ and the clinical ground truth Cup_{Clinic} is calculated as:

$$\% \text{ Error} = \left| \frac{Cup_{Clinic} - Cup_{Color/Level\text{-}set}}{Cup_{Clinic}} \right| \qquad (7)$$

The average cup detection error from color component analysis approach and threshold level-set approach is 10.18% and 14.23%, respectively. Then a graph is plotted for the clinical cup diameter with the detected cup diameter from the two methods, as shown in Figure 14.

It can be seen that the percentage error of cup diameter is more than the percentage error of disc diameter. The reason is the cup segmentation is more difficult than the disc segmentation due to the presence of high density vascular architecture in the region of the optic cup traversing the cup boundary. To compare our proposed method, the threshold level-set method takes more time to achieve the cup boundary detection. However, the percentage error of both methods shows that the threshold level-set method provides better results than the color component analysis method. Therefore, the threshold level-set method is chosen for determining CDR value.

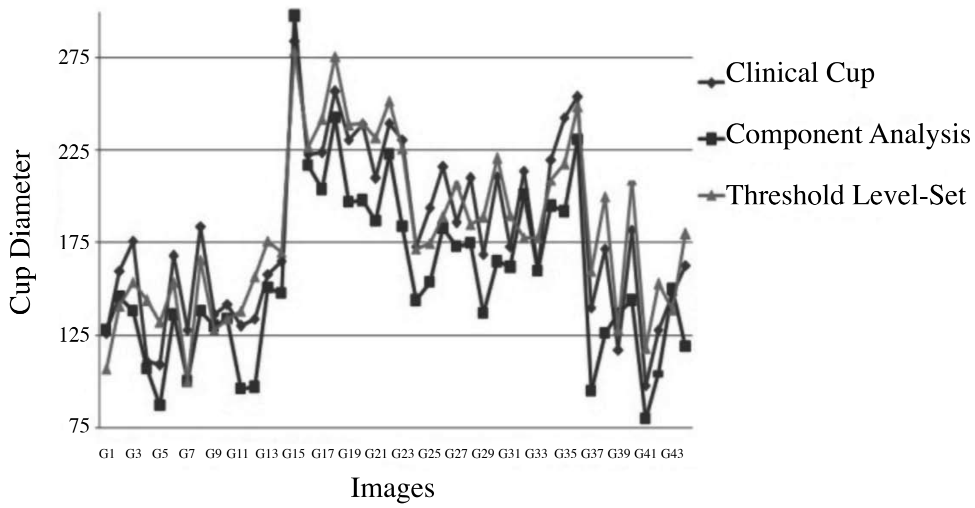

Fig. 14. Comparison of clinical cup detection and cup segmentation from color component analysis approach and threshold level-set approach.

4.3 The vertical cup-to-disc ratio (CDR)

Since CDR is an important indicator used for glaucoma detection, this metric is chosen to evaluate our results. The CDR is computed from the obtained cup and disc diameter from the chosen method. To evaluate the performance of the approach, the error E between the results obtained from the automated calculation $CDR_{Automated}$ and the clinical ground truth CDR_{Clinic} is calculated as:

$$E = CDR_{Clinic} - CDR_{Automated} \tag{8}$$

The distribution of E with respect to the sample images is shown in Figure 3.5. It can be observed from the results in Figure 15 that the maximum error for the CDR results obtained by our proposed method is less than 0.2 CDR units, with the average mean error calculated to be approximately 0.0611.

4.4 Glaucoma Diagnosis

To evaluate the effectiveness of our proposed method, Figure 16 is plotted. Figure 16 shows the detection of glaucoma based on our proposed method and the clinical method. The value of CDR which is more than 0.65 is used to assess a patient as a possible glaucoma case.

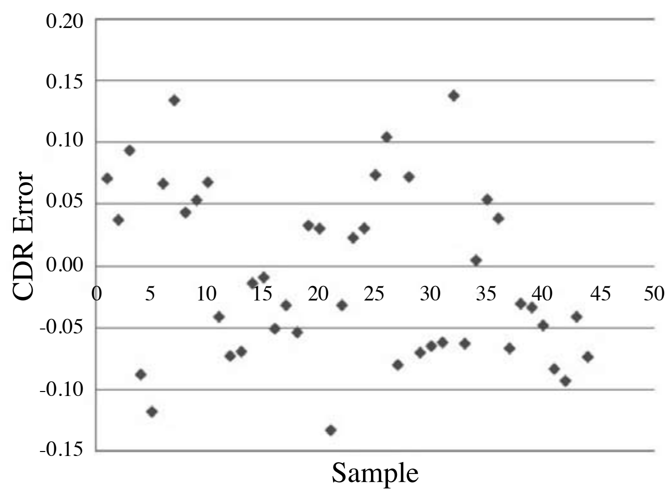

Fig. 15. Error between CDRAutomated and CDRClinical.

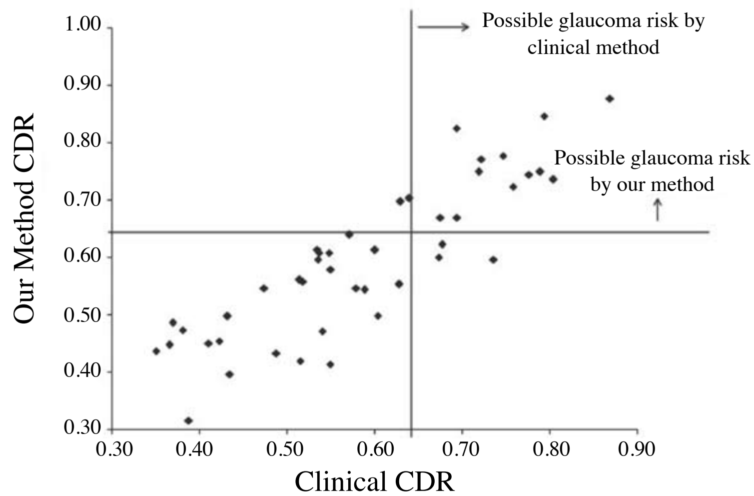

Fig. 16. Comparison between clinical CDR and our proposed CDR.

Table 1. Glaucoma classification confusion matrix

		Clinical Method: Normal	Clinical Method: Glaucoma
Our proposed method	Normal	27	3
	Glaucoma	2	12

93% Specificity	80% Sensitivity	89% Accuracy

Then, a confusion matrix is introduced to measure the performance of our proposed method. A confusion matrix contains three variables which are Sensitivity, Specificity, and Accuracy. According to this study, Sensitivity is defined as the percentage of glaucoma cases that is correctly identified as having glaucoma. Specificity is defined as the percentage of normal case that is correctly identified as not having glaucoma. Accuracy is the overall correctness of both normal cases and glaucoma cases.

From Figure 16, the result of a data set is shown in Table 1. This table shows the confusion matrix of glaucoma classification. The confusion matrix shows that 27 out of 29 normal cases are classified correctly. Glaucoma is classified correctly in 12 out of 15 cases. It shows that the Sensitivity of glaucoma classification is 80% which is considered as acceptable. Glaucoma classification has a high Specificity, up to 93%. The total accuracy is 89%.

5. Conclusion and Further Research

The cup to disc ratio (CDR) is an important indicator of the risk of the presence of glaucoma in an individual. In this study, we have presented a method to calculate the CDR automatically from fundus images. The image pre-processing is the first step to localize the optic disc and cup. The optic disc is extracted using an edge detection approach and a variational level-set approach separately. The optic cup is then segmented using a color component analysis method and threshold level-set method. After obtaining the contours, an ellipse fitting step is introduced to smoothen the obtained results. Using 44 images obtained from Mettapracharak hospital, the performance of our approach is evaluated using the proximity of the calculated CDR to the manually graded CDR. The results indicate that our approach provides 89% accuracy in glaucoma analysis. As a result, this study has a good potential in automated screening systems for the early detection of glaucoma.

The further developments for this study are to enhance the performance of the cup segmentation method by including a method of vessel detection and vessel inpainting. In addition, machine-learning techniques will be applied in order to find the suitable parameters in several formulas, including edge detection approach and threshold level set approach.

6. References

[1] World Health Organisation Media centre(April, 2011). Magnitude and Causes of Visual Impairment [Online]. Available:http://www.who.int/mediacentre/factsheets/

[2] P. Rojpongpan (March, 2009). Glaucoma is second leading cause of blindness[Online]. Available: http://www.manager.co.th/QOL/ViewNews

[3] Singapore Ministry of Health (October,2005). Glaucoma Clinical Practice Guideline [Online]. Available: http://www.moh.gov.sg/mohcorp/publications

[4] J. Liu, D. Wong, J. Lim, H. Li, N. Tan, Z. Zhang, T. Wong and R.Lavanya, ARGALI : An Automatic Cup-to-Disc Ratio Measurement System for Glaucoma Analysis Using Level-set Image Processing, Proc. IFMBE, pp. 559-562, 2009

[5] J. Liu, D. Wong, J. Lim, X. Jia, F. Yin, H. Li, and T. Wong, Optic cup and disk extraction from retinal fundus images for determination of cup-to-disc ratio, Industrial Electronics and Applications, pp. 1828-1832, June 2008

[6] D. Wong, J. Liu, J. Lim, X. Jia, F. Yin, H. Li, and T. Wong, Level- set based automatic cup-to-disc ratio determination using retinal fundus images in ARGALI, Engineering in Medicine and Biology Society, pp. 2266-2269, 2008

[7] S. Kavitha, S. Karthikeyanand Dr. Duraiswamy, Early Detection of Glaucoma in Retinal Images Using Cup to Disc Ratio, Computing Communication and Networking Technologies (ICCCNT), pp. 1-5, July 2010

[8] Wang, M.Y., Maurer, C.R., Jr., Fitzpatrick, J.M. and Maciunas, R.J., ”An automatic technique for finding and localizing externally attached markers in CT and MR volume images of the head”, IEEE Transactions on Biomedical Engineering, pp. 627-637, August 2002

[9] C. Li, C. Xu, C. Gui, and M. Fox, Level Set Evolution Without Re-initialization: A New Variational Formulation, Computer Vision and Pattern Recognition, Vol. 1, pp. 430-436, June 2005

[10] J. B. MacQueen, ”Some Methods for classification and Analysis of Multivariate Observations, Proceedings of 5-th Berkeley Symposium on Mathematical Statistics and Probability, Berkeley, University of California Press, pp. 281-297, 1967

[11] A. Fitzgibbon, M. Pilu and R. B. Fisher, Direct least-squares fitting of Ellipses, IEEE Transactions on Pattern Analysis and Machine Intelligence, pp. 476-480, 1999